Study of Periodicity-breaking Error-fields in the W7-X Stellarator

C. Nührenberg

IPP, EURATOM Association, Wendelsteinstr. 1, 17491 Greifswald, Germany

1 Introduction

During the construction of the Wendelstein 7-X stellarator (W7-X, [1]) in Greifswald, Germany, the fabrication und assembly of the magnet system are metrologically surveyed and the data is evaluated for an early detection of systematic and statistical deviations from the coil design [2]. Especially the statistical deviations, which are different for each of the winding packages, can cause magnetic-field errors destroying the fivefold symmetry of W7-X. A possibility to model their impact on W7-X plasmas is to study the magnetic perturbations as such and use the perturbed-equilibrium method [3, 4] to describe the periodicity-destroying error-fields. This work demonstrates that the perturbative approach replaces to a very good approximation standard, non-linear equilibrium calculations on the full torus. An example shows the effect of periodicity-breaking error-fields on a W7-X plasma with $\iota \approx 1$ near the magnetic axis and $\iota \approx 10/9$ near the plasma edge.

2 The W7-X high-ι variant

The W7-X magnet system comprises three coil subsystems, which are evenly distributed in ten half-modules: (i) fifty modular coils (five types, numbered $1,\ldots,5$ in the table), (ii) twenty planar coils (two types, labeled A and B), and (iii) ten control-saddle coils (one type, labeled S). In the W7-X standard case with $5/6 < \iota_{\mathrm{vac}} < 5/5$, the modular-coil currents are identical, e.g. 1.6 MA, and the planar auxiliary coils, which provide flexibility in rotational transform, carry no current. The current loads needed for a W7-X high-ι low-shear vacuum field with the rotational transform $5/5 < \iota_{\mathrm{vac}} < 10/9$ are given in the table on the right. Such a W7-X high-ι configuration with $\iota \gtrsim 1$ at the magnetic axis is especially susceptible for error-fields $B_{1n}^{m,-m}$ with low integer m. For an error-field study in the perturbed-equilibrium framework, the region interior to the unperturbed 10/9 island chain was reconstructed to a good approximation by a zero-β run of the VMEC equilibrium code [5]. The unperturbed triangular cross-section at $\varphi = 36^o$ is shown in the top frame of Fig. 1, with the VMEC flux surfaces (green), the result of field-line tracing in the vacuum field for the interior region (black), and the surrounding 10/9 island chain (red). An enclosed toroidal flux of $F_T = 1.9$ Vs in VMEC makes the magnetic field in MHD equilibrium and vacuum solution coincide, in particular the axis position (x in top frame of Fig. 1).

coil type	*current [MA]*
1	*1.92*
2	*1.92*
3	*1.696*
4	*1.248*
5	*1.248*
A	*-0.832*
B	*0.32*
S	*0*

In this work, a field perturbation is studied which destroys the five-fold periodicity of the device, but retains the stellarator symmetry. To this end, the currents in two neighbouring modular coils of type 2 (compare the table) are increased by 16 kA, whereas for two neighbouring type-4 coils (one on each side) the currents are descreased by the same amount. On the boundary of the toroidal domain, the difference between the

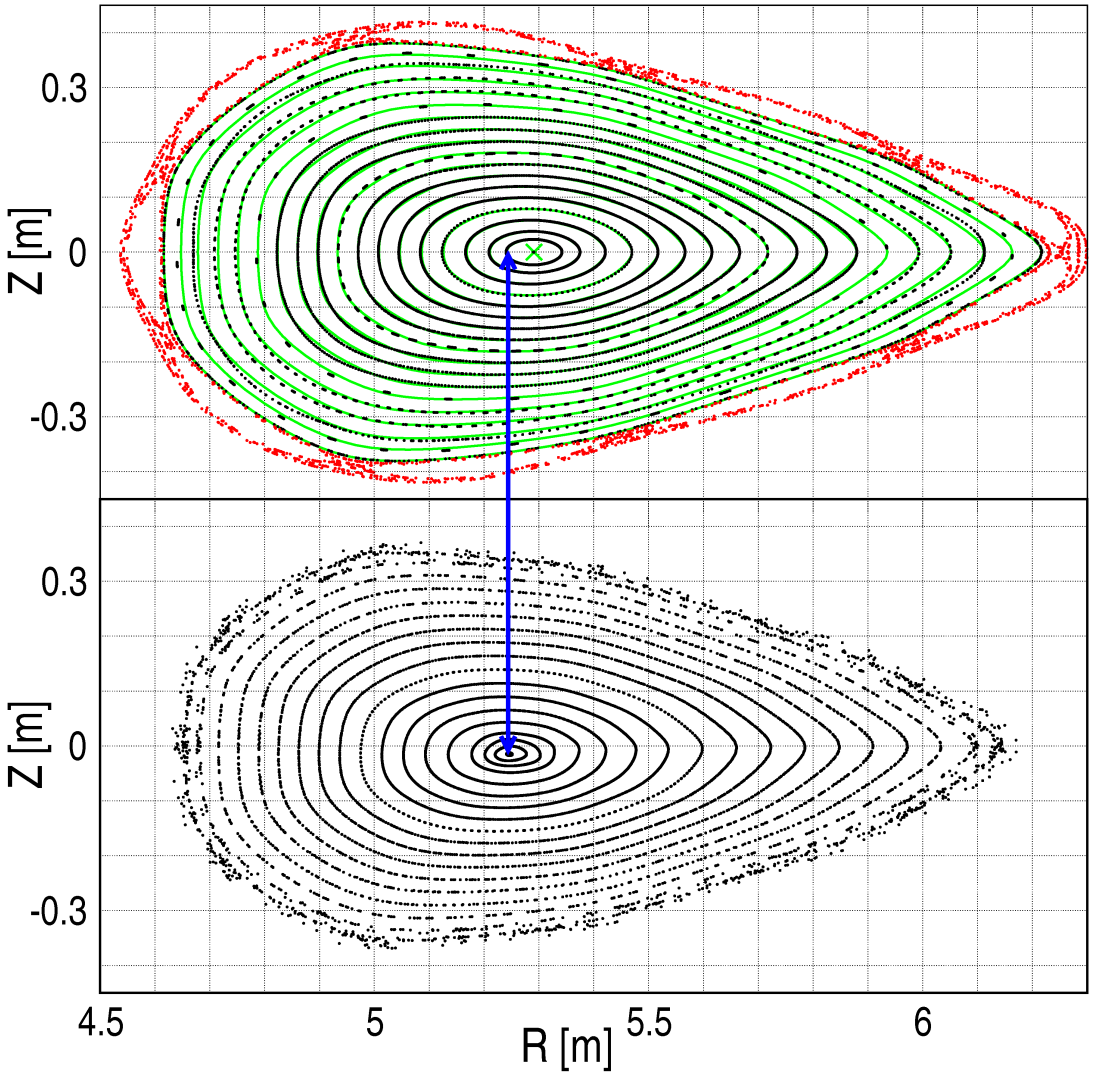

Figure 1: Triangular cross-section of a high-ι W7-X as determined by field-lining tracing. Top: unperturbed vacuum field from coil currents as given in Sec. 2. Bottom: perturbed field calculated by CAS3D-peq with displaced magnetic axis.

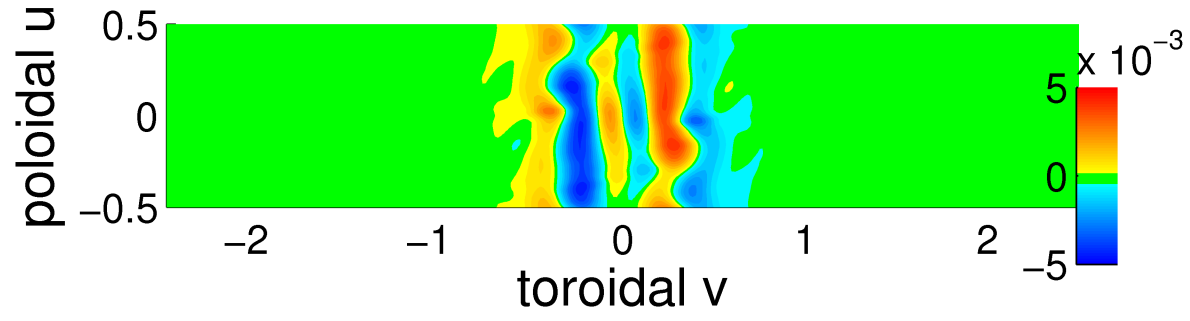

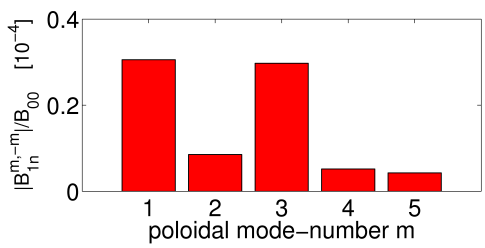

Figure 2: Top: Contours of the external B_{1n} [T] on the plasma boundary. The perturbation is centered around a bean-shaped cross-section, $\mathrm{v} = 0$, and is prominent in the field-period $-0.5 < \mathrm{v} < 0.5$. Left: $\iota = 1$ resonant harmonics of the external B_{1n} on the plasma boundary. The absolute values are shown relative to $B_{00} = 2.57$ T.

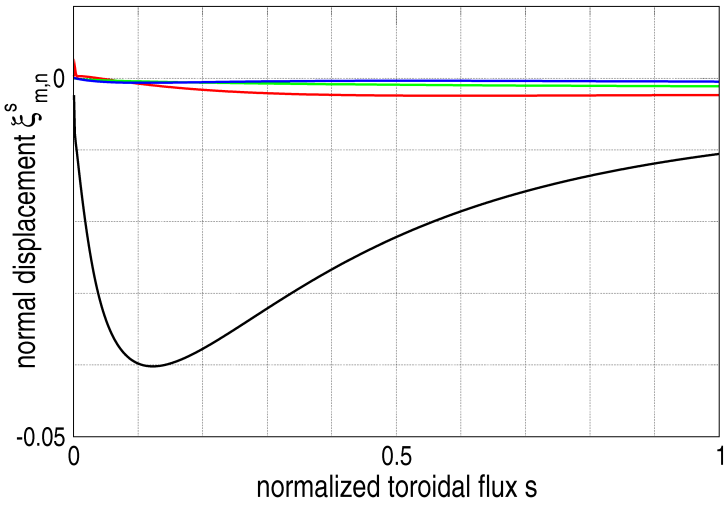

Figure 3: Normal displacement Fourier harmonics from CAS3D *which determines the perturbed equilibrium coming from the external field described in Fig. 2. The dominant four of 60 harmonics used in the computation are shown:* $m = 1, n = -1$ *(black);* $m = 3, n = -3$ *(red);* $m = 1, n = 0$ *(green);* $m = 2, n = -2$ *(blue).*

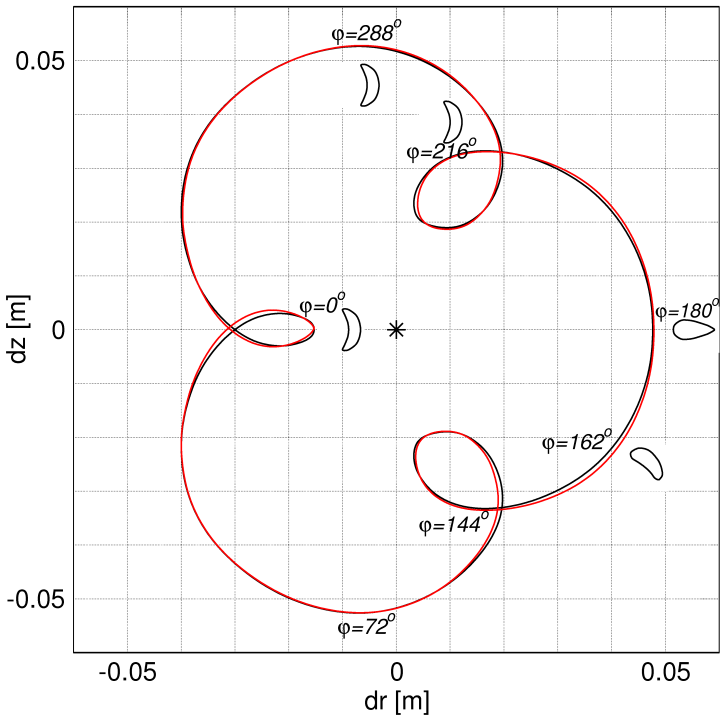

Figure 4: The deviation of the magnetic axis relative to the unperturbed axis (✳) from the vacuum-field (black) and from the CAS3D perturbed-equilibrium (red) calculations. The geometrical toroidal angle φ is the curve parameter, increasing by 72° in one of the five field-periods of W7-X. The varying shape of the plasma-cross-section is indicated, too.

two vacuum fields is sampled to find the normal component of the corresponding magnetic field perturbation, B_{1n}. Contours of the sampled B_{1n} are shown in the top frame of Fig. 2. The toroidal angle-like v increases by unity in one of the five field-periods, with $v = 0$ in the bean-shaped, $v = \pm 0.5$ in the triangular cross-section. $u = 0$ is on the outside of the torus, $u = \pm 0.5$ at the inside. With $|B_0| \approx 2.57$ T, the perturbation applied results in $\max|B_{1n}|/|B_0| \approx 0.3 \times 10^{-4}$ on the boundary (see bottom frame of Fig. 2). The dominant B_{1n} harmonics occur for $m = 1$ and $m = 3$. For this scenario, the maximum horizontal axis displacement is 0.048 m to the outside of the torus, the maximum vertical displacement is 0.052 m. The length of the magnetic axis is 39.6 m.

In Fig. 3, the dimensionless, free-boundary normal displacement is given which describes the corresponding perturbed equilibrium as calculated by the CAS3D code (compare the Appendix for a short description of the method). This displacement continuously matches the the external B_{1n} of Fig. 2. The computation was done using 701 radial mesh points and sixty perturbation harmonics. As shown in the bottom frame of

Fig. 1 for the triangular cross-section at $\mathrm{v} = 0.5$ (36^o), the geometry of the toroidal domain persists in general, the magnetic axis, however, is displaced. The deviation of the perturbed axis relative to the unperturbed axis is given in Fig. 4; the result from CAS3D (red) very well coincides with the data from the vacuum field (black). Along the axis, i.e. a field-line closing upon itself after ≈ 40 m in this case, the maximum error in the determination of the axis deviation by the CAS3D code is 0.0012 m, which is to be compared to a maximum axis deviation of 0.05 m in this scenario. This is especially interesting with the advent of diagnostical methods such as the close-range photogrammetry of the three-dimensional structures of magnetic fields in plasma devices. In the WEGA stellarator (Greifswald, Germany) such field-line measurements have been performed [6] visualizing field-lines on a length of ≈ 25 m with a spatial resolution of 0.005 m.

3 Summary

The perturbed-equilibrium method as implemented in the CAS3D code was successfully applied for studying the impact of a periodicity-destroying, external perturbation field on a W7-X configuration. In the high-ι variant studied, the axis dislocation caused by the chosen perturbation field and $\iota \approx 1$ near the magnetic axis was modeled to a very good approximation by CAS3D-peq. This result encourages comparisons with the recently introduced, three-dimensional, photogrammetric measurements of magnetic field-lines in plasma devices.

Appendix

A detailed description of the concept of perturbed equilibria is found in Refs. [3, 4]. A set of magnetic surfaces and two profiles, the rotational transform ι and the pressure p, define an unperturbed plasma state for which a small perturbation is considered. The perturbed equilibrium can be obtained from the unperturbed quantities (subscript 0), via the stationarity of $\delta^1 W + \delta^2 W = \int (\nabla p_0 - \vec{\jmath}_0 \times \vec{B}_0) \cdot \vec{\xi} \; \mathrm{d}^3 r - \frac{1}{2} \int \vec{\xi} \cdot \mathscr{F}[\vec{\xi}] \mathrm{d}^3 r$, which results in $\mathscr{F}[\vec{\xi}] = \vec{g}$. The ideal MHD force operator is $\mathscr{F}$, the displacement is $\vec{\xi}$, the magnetic field $\vec{B}$, and the current density $\vec{\jmath}$. The right-hand-side $\vec{g}$ derives from the perturbed plasma force $\vec{\xi} \cdot (\nabla p_0 - \vec{\jmath}_0 \times \vec{B}_0)$. Force balance, $\left[p + |\vec{B}|^2/2 \right]_{inside} = \left[p + |\vec{B}|^2/2 \right]_{outside}$, which must hold at any interface, and the continuity of the perturbed-magnetic-field normal component, B_{1n}, are the boundary conditions for the perturbed-equilibrium calculation.

References

[1] BOSCH, H.-S. et al., Construction of Wendelstein 7-X — engineering a steady-state stellarator, IEEE Trans. Plasma Sci. **38** (2010) 265.

[2] ANDREEVA, T. et al., Influence of construction errors on Wendelstein 7-X magnetic configurations, Fus. Eng. Design **84** (2009) 408.

[3] BOOZER, A. H., Perturbed plasma equilibria, Phys. Plasmas **6** (1999) 831.

[4] NÜHRENBERG, C. et al., Magnetic-surface quality in nonaxisymmetric plasma equilibria, Phys. Rev. Lett. **102** (2009) 235001.

[5] HIRSHMAN, S. P. et al., Three-dimensional free boundary calculations using a spectral Green's function method, Comput. Phys. Commun. **43** (1986) 143.

[6] DREWELOW, P. et al., Three-dimensional photogrammetric measurement of magnetic field lines in the WEGA stellarator, Rev. Sci. Instr. **80** (2009) 123501.